Viscous simulations of shock-bubble interaction and Richtmyer-Meshkov instability

Marion Capuano, Christophe Bogey, Peter D. M. Spelt

Viscous simulations of shock-bubble interaction and Richtmyer-Meshkov instability

M. CAPUANO [a], C.BOGEY [a], P.D.M SPELT [a,b]

a. Laboratoire de Mécanique des Fluides et d'Acoustique, UMR CNRS 5509, Ecole Centrale de Lyon, 69134 Ecully Cedex, France.
marion.capuano@doctorant.ec-lyon.fr
b. Département de Mécanique, Université Claude Bernard Lyon 1, 69622 Villeurbanne, France

Résumé :

L'interaction entre une onde de choc et une bulle ainsi que le dévelopement de l'instabilité de Richtmyer-Meshkov sont simulés à l'aide d'une méthode numérique explicite d'ordre élevé. Les simulations sont réalisées en résolvant les équations de Navier-Stokes complétées de deux équations d'advection gouvernant l'interface entre deux fluides. L'équation d'état raidie est utilisée afin de relier la pression à l'énergie totale d'un liquide ou d'un gaz. Deux écoulements diphasiques sont simulés en deux dimensions. Le premier concerne le développement d'une instabilité de Richtmyer-Meshkov suite au passage d'une onde de choc à travers l'interface entre de l'air et de l'hexafluorure de soufre (SF6). L'influence du raffinement du maillage sur la forme de l'instabilité est étudiée. Le second problème porte sur l'interaction d'une onde de choc plane et d'une bulle cylindrique contenant de l'hélium ou du chlorodifluorométhane (R22). Un diagramme spatio-temporel représente les positions des différentes ondes de pression créées au contact entre l'onde de choc et l'interface. Les résultats numériques obtenus pour les deux écoulements sont en accords avec les données et visualisations expérimentales.

Abstract :

Viscous simulations of shock-bubble interaction and Richtmyer-Meshkov instability are performed using an explicit high-order computational method. The simulations are performed by solving the Navier-Stokes equations associated with two convection equations governing the interface between two fluids. The stiffened equation of state is used to relate the pressure to the total energy of a liquid or a gas. Two-dimensional two-phase flows are considered. The first flow concerns the Richtmyer-Meshkov instability developed on a post-shocked interface between air and sulphur hexafluoride (SF6). The influence of the grid refinement on the instability shape is studied. The second problem deals with a shock wave propagating in air and hitting a cylindrical bubble filled with helium or chlorodifluoromethane (R22). A spatial-time diagram represents the locations of the various pressure waves generated from the interaction between the shock wave and the interface. For both simulations, the numerical results are in agreement with experimental data and visualizations.

Key words : finite differences, viscous, bubble, interface, shock wave

1 Introduction

Two-phase flows are encountered in many applications such as gas engine injection or cavitation phenomena. They present an interface between two fluids, which can be deformed by the propagation of pressure waves. In the present study, a computational method is used to simulate the interaction between interfaces and pressure waves including viscous effects [4]. Two-dimensional two-phase flows are considered. The first one contains a perturbed interface between air and SF6 which is impacted by a plane shock wave [6]. This shock-interface interaction leads to the generation of the Richtmyer-Meshkov instability providing a mushroom shape interface. The influence of grid refinement is shown on the instability shape and then on the temporal evolution of the width of the mushroom stem. The second flow considered in this work contains a plane shock wave propagating in air and impacting a cylindrical bubble filled with helium or R22 [5]. The locations of the various pressure waves and of the interface are plotted against time and compared with experimental data.

The present paper is organized as follows. The governing equations and the numerical methods are briefly detailed in Section 2. The results obtained for the two-dimensional flows are presented in Section 3. Concluding remarks and perspectives are finally provided in Section 4

2 Governing equations and numerical methods

In order to simulate compressible and viscous two-phase flows, the conservative Navier-Stokes equations associated with two advection equations governing the interface are solved [1, 9]. They are written as :

$$\begin{cases} \dfrac{\partial \rho}{\partial t} + \dfrac{\partial \rho u_i}{\partial x_i} = 0 \\ \dfrac{\partial \rho u_i}{\partial t} + \dfrac{\partial \rho u_i u_j}{\partial x_j} = \dfrac{\partial \sigma_{ij}}{\partial x_j} \\ \dfrac{\partial E}{\partial t} + \dfrac{\partial u_i E}{\partial x_i} = \dfrac{\partial}{\partial x_i}(\sigma_{ij} u_j) - \dfrac{\partial q_i}{\partial x_i} \\ \dfrac{\partial}{\partial t}\left(\dfrac{1}{\gamma - 1}\right) + u_i \dfrac{\partial}{\partial x_i}\left(\dfrac{1}{\gamma - 1}\right) = 0 \\ \dfrac{\partial}{\partial t}\left(\dfrac{\gamma B}{\gamma - 1}\right) + u_i \dfrac{\partial}{\partial x_i}\left(\dfrac{\gamma B}{\gamma - 1}\right) = 0 \end{cases} \tag{1}$$

where ρ is the density, u_i is the velocity component in the i-direction, E is the total energy and p is the pressure. The stress tensor σ_{ij} is for a compressible Newtonian fluid and the thermal conductivity vector q_i is computed from the Fourier's law.

In order to relate the pressure to the total energy of a liquid or a gas, the stiffened equation of state is used [7]. It is expressed as :

$$p = \frac{1}{1/(\gamma - 1)} \left(E - \frac{1}{2} \rho u_i^2 - \frac{\gamma B}{(\gamma - 1)} \right) \tag{2}$$

where γ and B are characteristic constant of each fluid.

In order to solve these equations, an explicit fourth-order finite difference scheme is used for spatial discretization [2]. It is centered over eleven points and has been designed to minimize the numerical dispersion error. Concerning time advancement, a six-stage Runge-Kutta algorithm is employed [2]. A sixth-order spatial selective filter is applied at each time step to remove grid-to-grid oscillations without

significantly impacting the high wavelengths. A discontinuity capturing methodology is used to capture shock waves and deformable fluid/fluid interfaces which can be encountered within compressible two-phase flows [3, 4].

3 2D Simulations

3.1 Richtmyer-Meshkov instability

The first case considered in this study concerns the Richtmyer-Meshkov instability generated on a post-shocked interface between air and sulphur hexafluoride (SF6). This flow has been experimentally investigated by Jacobs and Krivets [6]. Initially, the two gases are stationary in a vertical shock tube. Then the shock tube is horizontally shaken in order to perturb the interface. Finally, a shock wave propagating in air with a Mach number $M = 1.29$, impacts the perturbed interface. These experimental conditions are used to set the parameters of the simulation. Initially, the shock is located at the abscissa x_s and the position of the interface x_{int} is described using a cosine profile with a wavelength $\lambda = 59$ mm and an amplitude $a = 2.9$ mm. Experimentally, the distance between the two walls of the shock tube is larger than the perturbation wavelength. Consequently, multiple instabilities develop on the interface. In the simulation, only one instability is generated using periodic boundary conditions spaced by one wavelength λ. Radiation conditions are imposed at the upstream and downstream extremities of the domain. The initial conditions for the density, the axial velocity, the pressure and the variables γ and B are the following :

$$(\rho, u_x, p, \gamma, B) = \begin{cases} (2.2997, 136, 178670, 1.27, 0) & \text{for } x \leq x_s \\ (1.4933, 0, 101325, 1.27, 0) & \text{for } x_s < x \leq x_{int} \\ (6.0156, 0, 101325, 1.0984, 0) & \text{for } x > x_{int} \end{cases}$$

Five uniform grids have been considered. They contain 64, 128, 256, 512 and 1024 mesh cells in the y-direction which is normal to the walls, and are denoted by *ny64*, *ny128*, *ny256*, *ny512* and *ny1024*, respectively. The Courant-Friedrich-Lewy number based on the speed of sound in air, is set to $CFL = 0.9$.

The results obtained at time $t = 5.86$ ms after the contact between the shock and the interface are presented in the Figure 1. The experimental visualization is in the first column. The numerical density fields presented in the three next columns are obtained on the meshes *ny128*, *ny256* and *ny512*. The air density is in gray and the SF6 density is in black. The Richtmyer-Meshkov instability results in a finger of SF6 which penetrates the air. This finger grows and leads to a mushroom shape interface. The shape of the instability is well predicted by the three simulations. However, the small scales in the mixing zones at the left-hand side and right-hand side of the mushroom stem are better resolved on the mesh *ny512*. The temporal evolution of the width of the stem W, estimated at the half distance between the bottom and the top of the mushroom, is represented in the Figure 2. As the instability grows, the mushroom stem becomes longer and thinner. Therefore, the width of the stem decreases. Negligible differences are observed between the solutions estimated on the two finest meshes *ny512* and *ny1024*. Consequently, the simulation computed on the mesh *ny512* is converged with respect to the grid.

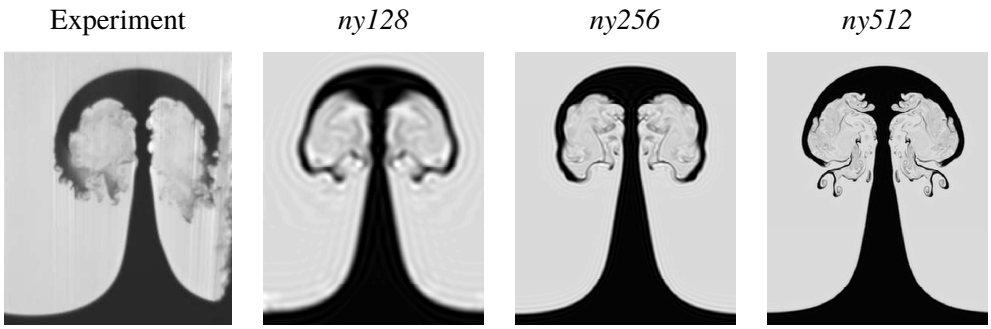

FIGURE 1 – Richtmyer-Meshkov instability on the air-SF6 interface at time $t = 5.86$ ms, with respect to the experimental conditions stated in the main text. The experimental visualisation from [6] is presented in the first column. The density fields are obtained using the meshes *ny128* in the second column, *ny256* in the third column and *ny512* in the fourth column.

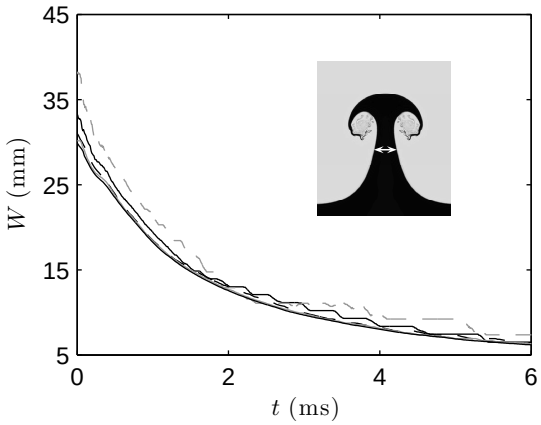

FIGURE 2 – Temporal evolution of the width of the stem W estimated at the half-distance between the top and the bottom of the mushroom, using the meshes - - - *ny64*, ····· *ny128*, - - - *ny256*, — *ny512* and — *ny1024*.

3.2 Shock-bubble interaction

The second two-phase flow considered in this study is taken from the experiments of Haas and Sturtevant [5]. It consists of a cylindrical bubble of diameter $D = 5$ cm hit by a plane shock wave propagating in air with a Mach number $M = 1.22$. Initially, the shock is located at abscissa x_s and propagates from the right to the left of the domain along the horizontal direction x. The walls of the shock tube are spaced by 89 mm and the bubble is centered on the vertical axis y. Two simulations are performed. In the first case the bubble is filled with helium, which is lighter than air, and in the second case it is filled with chlorodifluoromethane (R22), which is heavier than air. The initial conditions for the density, the axial velocity, the pressure and the variables γ and B are :

$$(\rho, u_x, p, \gamma, B) = \begin{cases} (1.664, -114, 159059.98, 1.4, 0) & \text{for } x > x_s \\ (1.2098, 0, 101325, 1.4, 0) & \text{in air, for } x \leq x_s \\ (0.2204, 0, 101325, 1.6451, 0) & \text{inside the helium bubble} \\ (3.374, 0, 101325, 1.1847, 0) & \text{inside the R22 bubble} \end{cases}$$

The simulations are carried out on a uniform mesh containing 2.9×10^6 cells with a grid spacing equal to $\Delta x/D = 2.5 \times 10^{-3}$. The CFL number is set to 0.9 and is estimated from the highest speed of sound encountered within the flow. Periodic boundary conditions are used to model the walls of the shock tube, and radiations conditions are imposed at the upstream and downstream extremities of the domain. The results obtained for both cases are presented in the Figure 3. The experimental shadow-photographs [5] are in the lower-half picture and the numerical Schlieren pictures are in the upper-half picture. The dashed circle indicates the initial position of the bubble. The solutions obtained for the helium bubble at time $t = 245$ μs are presented in the Figure 3(a). The bubble is advected downstream after the impact of the shock wave. The upstream interface penetrates the bubble leading to a kidney-shaped interface. A vorticity field rotating clockwise in the upper-half domain and couterclockwise in the lower-half is generated. The results obtained for the R22 bubble at time $t = 247$ μs are presented in the Figure 3(b). The upstream interface, located at the center of the dashed circle is advected downstream and is almost not deformed. The downstream interface, located at the left of the dashed circle, present a spike on the axis of symmetry. This bubble shape is due to the vorticity field which is reversed from the previous case with the helium bubble. For both cases, the numerical results are in agreement with experimental visualizations. The various transmitted, refracted and reflected pressure waves are correctly propagated and the interface deformations are well predicted by the simulation.

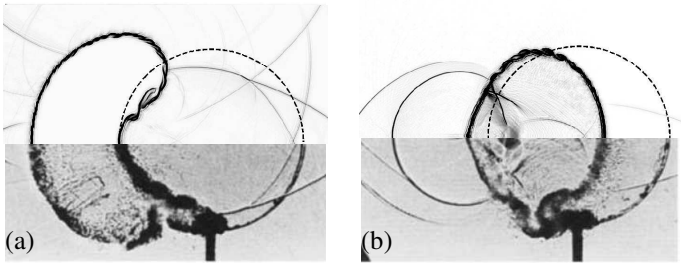

FIGURE 3 – Numerical Schlieren pictures (upper-half picture) and experimental shadow-photographs (lower-half picture) [5] obtained (a) with a helium bubble at time $t = 245$ μs and (b) with a R22 bubble at time $t = 247$ μs.

In Figure 4, the locations of the pressure waves and of the R22 bubble interfaces are plotted against time. The positions of the upstream and downstream interfaces are in dashed lines. The locations of the refracted and transmitted waves are represented by a gray solid line and by black dashed and dotted lines, respectively. They are computed on the bubble axis of symmetry. The incident shock wave positions (black solid line) are estimated on the horizontal axis at half-distance between the top of the bubble and the upper wall. The black circles represent the experimental data of Haas and Sturtevant [5]. After the impact between the incident shock wave and the upstream part of the interface at time $t = 0$, the interface is advected downstream and a refracted wave is generated, and propagates inside the bubble. Then, the refracted wave impacts the downstream part of the interface at $x = 50$ mm and at time $t = 194$ μs. This interface is advected downstream and a pressure wave is transmitted outside the bubble. The numerical results are in agreement with the experimental data. The positions, and the speeds of the various pressure waves and of the interfaces are well predicted by the simulation.

4 Concluding remarks

Two-dimensional viscous and compressible flows are simulated using an explicit high-order computational method which consists in solving the Navier-Stokes equations associated with two advection

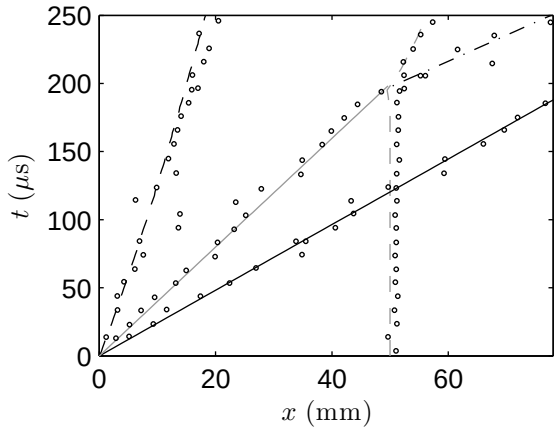

FIGURE 4 – Space-time diagram of the interaction of a plane shock wave at Mach $M = 1.22$ with an R22 cylindrical bubble. Locations of the — incident shock wave, — refracted wave, -·-·- transmitted wave - - - upstream interface and - - - downstream interface ; ○ experimental data [5]

equations governing the interface. Firstly, a simulation of the Richtmyer-Meshkov instability between air and SF6 is performed. The interface initially perturbed is deformed by the interaction with the shock wave, providing a mushroom shape. The influence of grid refinement is shown on the on the instability shape and on the temporal evolution of the width of the mushroom stem. The grid spacing of the mesh *ny512* is sufficiently fine to accurately solve this flow. Secondly, the interaction between a shock wave and a cylindrical bubble filled with helium or R22 is considered. In both simulations, the numerical results are in agreement with experimental data. The interaction of the pressure waves with the interface are well resolved leading to accurate deformations of the interface. The numerical method correctly propagates the various pressure waves, such as reflected, refracted and transmitted waves which are generated at the contact with the interface. In further studies, a spherical collapsing bubble filled with air and surrounded by water will be considered [8].

Acknowledgements

This work was performed using HPC resources of P2CHPD (Pôle de Calcul Hautes Performances Dédiés) of Université Lyon 1 (Mésocentre FLMSN). This work was performed within the framework of the Labex CeLyA of Université de Lyon operated by the French National Research Agency (ANR). The authors thank Dr Stephen J. Shaw for interesting discussions.

References

[1] R. Abgrall and S. Karni, Computations of compressible multifluids, J. Comput. Phys., 169(2) :594-623, 2001.

[2] C. Bogey and C. Bailly, A familiy of low dispersive and low dissipative explicit schemes for flow and noise computations, J. Comput. Phys., 194 :194-214, 2004.

[3] C. Bogey, N. De Cacqueray and C. Bailly, A shock-capturing methodolodgy based on adaptative spatial filtering for high-order non-linear computations, J. Comput. Phys., 228 :1447-1465, 2009.

[4] M. Capuano, C.Bogey and P.D.M. Spelt, Numerical simulations of viscous and compressible two-phase flows using high-order schemes, 9th International Conference on Multiphase Flows, Firenze, 2016.

[5] J-F. Haas and B. Sturtevant, Interaction of weak shock waves with cylindrical and spherical gas inhomogeneities, J. Fluid Mech., 181 :41-76, 1987.

[6] J.W. Jacobs and V.V. Krivets, Experiments on the late-time development of single-mode Richtmyer-Meshkov instability, Phys. of Fluids, 034105, 2005.

[7] S. Jolgam, A. Ballil, A. Nowakowski and F. Nicolleau, On equations of state for simulations of multiphase flows, World Congress on Engineering July 4-6, London, UK., 3 :1963-1968, 2012.

[8] S.J. Shaw and P.D.M Spelt, Shock emission from collapsing gas bubbles, J. Fluid. Mech., 646 :363-373, 2010.

[9] K-M. Shyue, An efficient shock-capturing algorithm for compressible multicomponent problems, J. Comput. Phys., 142 :208-242, 1998.